 doi:10.20944/preprints202011.0218.v1

Composite ferroelectric membranes based on vinylidene fluoride-tetrafluoroethylene copolymer and polyvinylpyrrolidone for wound healing: a pilot study

T. S. Tverdokhlebova[1], L.S. Antipina[2], V.L. Kudryavtseva[1,3], K.S. Stankevich[1,4], I.M. Kolesnik[1], E.A. Senokosova[5], E.A. Velikanova[5], L.V. Antonova[5], D. V. Vasilchenko[2], G. T. Dambaev[2], V.M Bouznik[6,7], E.N. Bolbasov[1,]*

1. Tomsk Polytechnic University, Tomsk, Russian Federation.

2. Siberian State Medical University, Tomsk, Russian Federation.

3. Queen Mary University of London, London, United Kingdom.

4. Montana State University, Bozeman, United States.

5. Research Institute for Complex Issues of Cardiovascular Diseases, Kemerovo, Russian Federation.

6. All Russian Scientific Research Institute of Aviation Materials, Moscow, Russian Federation.

7. Tomsk State University, Tomsk, Russian Federation.

**- Corresponding author. E-mail address: Ebolbasov@gmail.com (E.N. Bolbasov)*

Abstract

Herein, we report results of the study of the composite scaffolds based on vinylidene fluoride-tetrafluoroethylene copolymer (VDF-TeFE) and polyvinylpyrrolidone (PVP) produced by electrospinning and their application as a wound-healing material. The physicochemical properties of ferroelectric composite polymer scaffolds depending on the content of PVP (in the range from 0 to 50 wt %) including morphology, composition and crystalline structure were studied. The cytotoxicity of materials and the proliferative activity of cells during their cultivation on the surface of formed scaffolds are reported. It has been found that the optimal PVP content in the VDF-TeFE composite scaffolds is 15 wt%. On a model of a full-thickness contaminated wound in vivo, it was shown that piezoelectric scaffolds based on VDF-TeFE copolymer containing 15 wt% PVP provide better wound healing results in comparison with standard gauze dressings impregnated with a solution of an antibacterial agent.

Keywords: Ferroelectrics, Composite, Membranes, Polyvinylpyrrolidone, Wound healing.

1. Introduction.

Despite antibacterial treatment, infectious complications of wound continue to be a significant factor contributing to patient morbidity and poor healing outcomes. Damaged skin cannot effectively perform protective, immune, respiratory, metabolic, thermoregulating, receptor and other functions. It may provoke not only local complications but systemic pathological changes in the body [1].

 doi:10.20944/preprints202011.0218.v1

Wound healing is a long-term multi-stage process which may be inhibited by external environment [2]. Modern concepts of the pathophysiology of the wound healing state several basic requirements for wound dressings including: physical protection of the wound from external injury; inhibition of bacterial invasion; wound exudate absorption; maintaining the physiological temperature and humidity; gas and liquid transport; mechanical flexibility; easy removal without adhesion to the wound and biocompatibility [3]. These requirements are proven to prevent tissue dehydration and cell death, improve intercellular interaction and angiogenesis and the wound healing process. Despite the variety of modern materials used for wound healing (foams, hydrogels, sprays, etc.) [4], electrospun polymer non-wowen membranes [5–7] meet all the necessary requirements [3] being the most promising dressing material.

Piezoelectric properties of collagen [8], the most common fibrillar protein that forms dermis, triggered investigations directed towards devices and materials capable of accelerating tissue regeneration processes through electrical stimulation [9]. Closer attention received ferroelectric and piezoelectric polymer materials and their application in reconstructive surgery [10]. Considerable interest in these is due to the possibility of electrical stimulation of tissue regeneration processes via membrane mechanical deformations from cell, tissues or organs [11]. This approach does not require external source of electrical energy, batteries or electrodes, excluding the possibility of accumulation of electrolysis products in tissues [12].

Due to the higher electronegativity of fluorine (F) comparing to carbon (C) and hydrogen (H) in polyvinylidene fluoride (PVDF) and its copolymers with tetra- (TeFE) and trifluoroethylene (TrFE), a certain conformation of the macromolecule results in a dipole moment in polymer chain directed perpendicular to its axis. PVDF the most electrically active piezoelectric polymer [13]. Currently, the application of PVDF elecrospun scaffolds as a wound healing material is being actively studied [14–17].

Despite the obvious advantages, such membranes suffer from the high hydrophobicity, which limits the absorption of wound exudate and low encapsulation efficiency due to its the high chemical resistance [18]. The problem can be solved by the development of composite membranes based on fluoropolymer piezoelectrics.

In this work, we report results of our study of the composite membranes based on vinylidene fluoride-tetrafluoroethylene copolymer (VDF-TeFE) and polyvinylpyrrolidone (PVP) produced by electrospinning and their application as a wound healing material.

2. Materials and Methods

2.1 Preparation of VDF-TeFE/PVP membranes by electrospinning

Preprints (www.preprints.org) | NOT PEER-REVIEWED | Posted: 5 November 2020 doi:10.20944/preprints202011.0218.v1

A VDF-TeFE copolymer (Halopolymer, Russia), polyvinylpyrrolidone (PVP, Mn=1.25×10^5 g/mol, Kollidon® 90 F, BASF, Germany) and demitylformamide (DMF, Ecros-1, Russia) were used for solution preparation. Membranes were produced by the electrospinning. Five types of spinning solutions were prepared with a mass ratio of VDF-TeFE/PVP polymers of 100/0, 95/5, 85/15, 75/25, 50/50 %. The total concentration of polymers in solution was 5 wt.% for all samples. Polymers were dissolved in a sealed glass reactor at a temperature of 40 °C with the constant stirring until a homogeneous transparent solution was obtained. The resulting solution was cooled to the room temperature.

The viscosity of the spinning solutions was measured using SV-10 viscometer (AND, Japan). The conductivity of the spinning solutions was measured using an InoLab Cond 7319 conductometer with a TetraCon 325 measuring cell (WTW, Germany). The viscosity and conductivity measurements of the spinning solutions were carried out at a temperature of 24°C.

A commercially available NANON 01A installation (MECC Co., Japan), equipped with a cylindrical assembly collector with a diameter of 50 mm and a length of 200 mm, was used for the formation of nonwoven materials. The distance between the dope injector (22G needle) and the assembly manifold was 150 mm. The voltage at the injector is 25 kW. The flow rate of the dope solution was 1.8 mL/hour, assembly speed was 50 rpm.

2.2. Investigation of physicochemical properties of membranes

Scanning Electron Microscopy (SEM)

The morphology of the samples was investigated by SEM using a JCM-6000 instrument (JEOL, Japan). Prior to the investigation, samples were coated with a thin gold layer by the magnetron sputtering system (SC7640, Quorum Technologies Ltd., UK). The fiber diameter was determined from SEM images captured in five fields of view using ImageJ 1.38 software (National Institutes of Health, USA). The average diameter was determined from at least 120 fibres.

Energy-dispersive spectroscopy (EDS)

Chemical composition of the membranes was analyzed using energy-dispersive spectroscopy (EDS) (JEOL JED 2300, Japan). The semiquantitative chemical composition of the membrane was calculated by the method of three corrections: for the average atomic number, absorption, and fluorescence.

Gas Chromatography (GC)

The study of the residual DMF content in the membranes was carried using Kristall 5000 chromatograph with a flame-ionization detector (Khromatek, Russia) equipped with a ZB-5MS

Preprints (www.preprints.org) | NOT PEER-REVIEWED | Posted: 5 November 2020 doi:10.20944/preprints202011.0218.v1

column (30 m×0.25 mm×0.25 μm). To determine the DMF content 100 ± 5 mg of each sample were dissolved in 10.0 ± 0.1 ml of acetone. The following parameters were used: the volume of the injected sample -1 μl, the evaporator temperature - 222 ° C; detector temperature - 250 °C; thermostat temperature - 90 ° C; inlet pressure - 100 kPa; flow rate - 10 mL/min.

Study of the structure of VDF-TeFE copolymer in composite membranes

Ferroelectric properties of PVDF and its copolymers are determined by the conformation of macromolecules and as a result by its crystalline structure. There are three main polymorphs (α, β, γ). α-phase is characterized by a monoclinic lattice in which chain ($TGTG^-$) conformation have opposite dipole moments, so in general it is nonpolar. γ-phase contains a weakly polar cell with a chain ($T_3GT_3G^-$) conformation. β-phase is the most electroactive and is characterized by orthorhombic lattice with polar cell in which the chain has a planar zigzag (*TTT*) conformation [19]. The presence of polymorphic conformations and crystal structures typical of the paraelectric and ferroelectric phases allows determining their presence, using techniques such as XRD and FITR [20] .

Fourier Transform Infrared spectroscopy (FTIR)

The conformation of macromolecules VDF-TeFE in composite membranes was investigated using Attenuated Total Reflectance (ATR) Fourier Transform Infrared spectroscopy (FTIR) (Tensor 27, Bruker) with ATR attachment (PIKE MIRacle, Bruker) on the crystal ZnSe. Investigations were carried out in the spectral range of 500–2000 cm^{-1} with a resolution of 2 cm^{-1}.

X-ray diffraction analysis (XRD)

The crystal structure copolymer VDF-TeFE in composite membranes was investigated using X-ray diffraction analysis (XRD) (Shimadzu 6000, Japan). The samples were exposed to a monochromatic Cu Kα (1.54056 Å) radiation.

2.3. Investigation of biomedical properties of membranes

Adhesion, viability and proliferative activity of cells

The study of the interaction of the obtained membranes with cells *in vitro* was carried out using human dermal fibroblasts. For that 19 mm diameter sterile samples were placed into the well of 24-well plate and fixed with 0.6% agarose solution (Helicon, USA). For each well 1 mL of cell suspension containing 10^5 cells, DMEM (Sigma-Aldrich, USA) supplemented with 10% fetal calf serum (Gibco), 1% HEPES buffer (Gibco), 1% L-Glutamine – Penicillin – Streptomycin solution (Gibco) and 0.4% amphotericin B (Gibco) was added. The cells were cultured for 6 days using a

Preprints (www.preprints.org) | NOT PEER-REVIEWED | Posted: 5 November 2020 doi:10.20944/preprints202011.0218.v1

CO_2 incubator (Sanyo, Japan) in an atmosphere containing 5% CO_2 at temperature of 37°C and a humidity of 95%.

The absolute number of cells per 1 mm^2 of the surface and the relative content of dead cells was evaluated using fluorescence microscopy using Axio Observer Z1 inverted microscope (Carl Zeiss, Germany). Cells were stained with ethidium bromide (Sigma Aldrich, USA) 0.03 mg / mL (orange staining of nuclei of dead cells) and Hoechst 33342 (Sigma Aldrich, USA) 2 μg / mL (blue staining of nuclei of all adhered cells). The dyes were applied to the samples 3 min before microscopy. For better visualization of adhered cells, the cell membrane was stained with a PKH26 membrane dye (Sigma Aldrich, USA) with concentration of 2 μg/mL.

The proliferative activity of the adhered cells was evaluated using the Click-iTTM Plus EdU Alexa FluorTM 488 Imaging Kit (# C10637, Thermo Fisher Scientific Inc., USA). Studies of the proliferative activity of adhered cells were carried out using a confocal laser scanning microscope LSM 700 (Carl Zeiss, Germany). Cells were counted using the Image J 1.38 software (National Institutes of Health, Bethesda, USA) using 10 different fields of view at x200 magnification.

Studies of cell adhesion and proliferative activity were performed on 5 samples of each of the studied groups in triplicate using 10 randomly selected fields of view for each group. Cells cultured without a material were used as a control.

Composite membranes *in vivo* full-thickness contaminated wound healing

The wound healing activity of membranes was studied in 20 adult Wistar rats (body weight 180-200 g). An infected full-thickness contaminated wounds were formed. Rats were anesthetized and a rectangular excision area (20 × 20 mm) was cut on each animal. The edges of the wounds and underlying muscles were crushed with a Kocher's forceps. After that, microbial suspension containing 10^6 CFU of *Staphylococcus aureus* was applied topically to the wound area. The surface of the wound was covered with plastic wrap for 72 hours to form an acute inflammation. Animals were divided into two groups of 10 animals in each group. For the animals of the first group, a gauze bandage soaked in an aqueous solution of chlorhexidine (Kemerovo pharmaceutical factory, Russia) was applied to the wound surface. For animals of the second group the wound surface was covered with a VDF-TeFE membranes containing 15% PVP. The dressings were changed on 3, 5 and 7 days of the experiment.

Macroscopic photographs (digital camera EOS 250D, Canon, Japan) were used to evaluate healing activity of membranes. For histological analyses, the tissue samples were harvested from the region of interest. Samples were fixed in formalin and processed for histopathological

 doi:10.20944/preprints202011.0218.v1

observation. Prepared 5 μm-thick sections section of tissues were stained with hematoxylin and eosin and studied using transmission light microscopy (Axioscop40, Carl Zeiss).

The study was carried out in accordance with the principles of humane treatment of laboratory animals described in [21]. Prior to investigation all samples were sterilized in ethylene oxide atmosphere using a gas sterilizer AN4000 (Andersen Sterilisers, UK).

2.4 Statistics

The data were analyzed with Origin 9.0 (OriginLab, USA) software using the one-way ANOVA with Tukey's correction. The difference was considered significant at a significance level of $p<0.05$.

Preprints (www.preprints.org) | NOT PEER-REVIEWED | Posted: 5 November 2020 doi:10.20944/preprints202011.0218.v1

3. Results and Discussion

The morphology of the formed VDF-TeFE membranes and composite membranes with PVP content 50 % is shown in Figure 1.

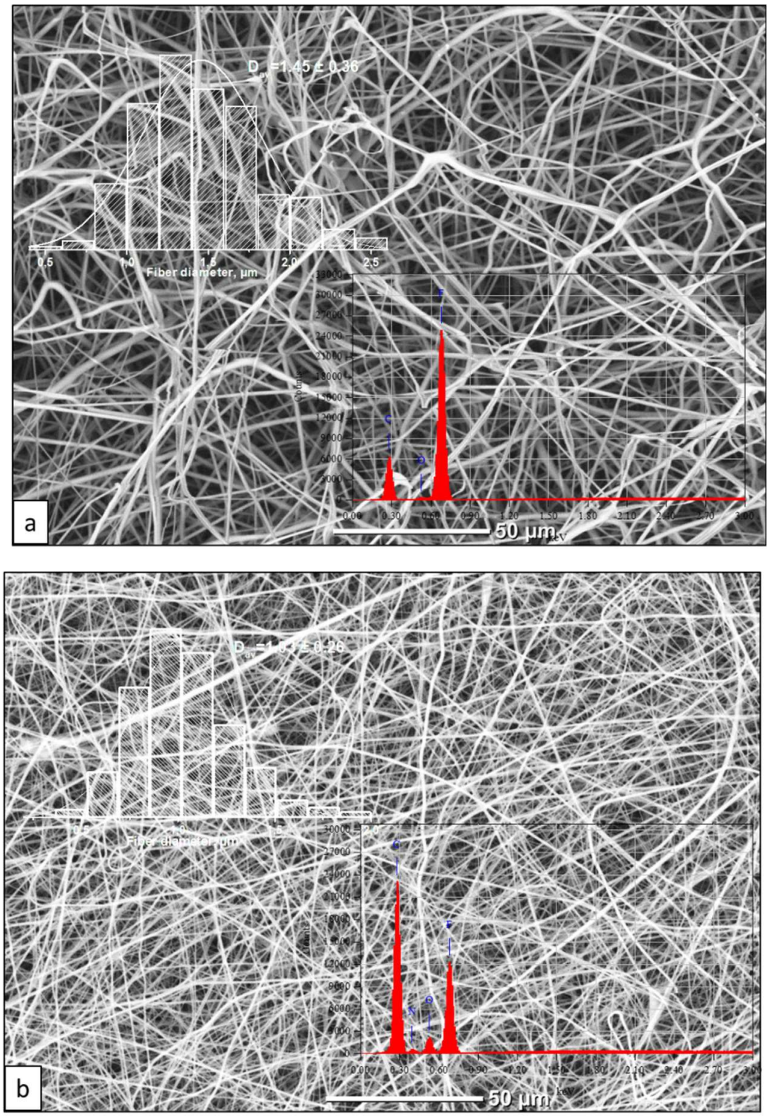

Figure 1. SEM images of VDF-TeFE membranes with different PVP content: a-0 %, b-50 %.

Regardless of the PVP content in the spinning solution, all the membranes are formed by cylindrical fibers of regular shape, randomly intertwining with each other. However, an increase in the PVP content in spinning solutions leads to a decrease of the fiber diameter from 1.45 ± 0.36 to 1.03 ± 0.26 μm due to a decrease in conductivity and dynamic viscosity of the solutions (Table 1.) The observed decrease in the dynamic viscosity is attributed to a lower content of the polymer with higher molecular weight in the mixture. Moreover, the solution conductivity drop from 2.84±0.02 to 1.50±0.04 μS/cm, accompanied by a decrease of the spinning solution viscosity, is probably induced by intermolecular interaction leading to the formation of complexes between the polymers and the solvent.

Preprints (www.preprints.org) | NOT PEER-REVIEWED | Posted: 5 November 2020 doi:10.20944/preprints202011.0218.v1

Table 1. Dynamic viscosity, conductivity of spinning solutions, mean fiber diameter in formed membranes.

PVP, %	Dynamic viscosity, mPa×s	Conductivity, μS/cm	Mean fiber diameter, μm
0	845 ± 11	2.84 ± 0.02	1.45 ± 0.36
5	725 ± 14	2.66 ± 0.02	1.41 ± 0.35
15	622 ± 7	2.42 ± 0.03	1.37 ± 0.34
25	492 ± 16	2.06 ± 0.02	1.30 ± 0.32
50	227 ± 9	1.50 ± 0.04	1.03 ± 0.26

Chemical composition of the membranes was analyzed using energy-dispersive spectroscopy. The chemical composition of VDF-TeFE membranes without PVP is mainly represented by carbon (C) and fluorine (F). Low amount of oxygen (O) may be attributed to the presence of residual DMF used as a solvent for preparation of spinning solutions (Table 2).

Table 2. Elemental composition of VDF-TeFE membranes with different PVP content.

PVP content, %	Elemental composition, mass %				Residual DMF, ppm
	C	O	F	N	
0	44.5±0.7	1.0±0.2	54.6±0.7	-	762 ± 48
5	45.8±0.5	1.9±0.3	52.4±0.8	-	1195 ± 98
15	38.4±1.1	3.7±0.4	46.0±1.7	11.9±0.2	1521 ± 75
25	40.6±1.2	5.4±0.6	39.7±2.1	14.3±0.3	1912 ± 120
50	44.6±0.5	9.2±0.3	27.0±1.3	19.2±0.6	2423 ± 136

An increase of the PVP concentration in spinning solutions leads to an increase in the content of oxygen (O) and nitrogen (N) in the formed membranes (Table 2). These elements are presented in the composition of both PVP and DMF. At the same time, an increase of the PVP amount leads to higher DMF content in the samples (Table 2). Probably, the observed increase in the DMF content in the formed composite samples, as well as a decrease in the conductivity of spinning solutions is evidence of the formation of complex between PVP and DMF [22].

FTIR spectra of the studied membranes VDF-TeFE scaffolds with different PVP content are shown in Figure 3.

Preprints (www.preprints.org) | NOT PEER-REVIEWED | Posted: 5 November 2020 doi:10.20944/preprints202011.0218.v1

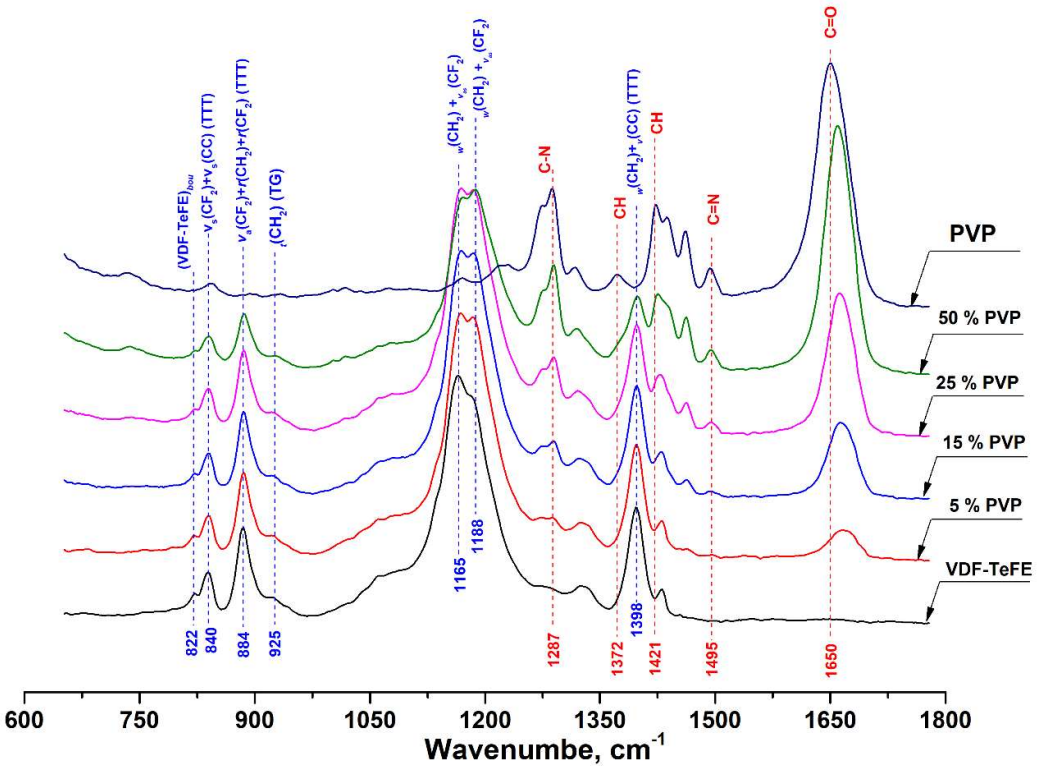

Figure 2. FTIR spectra of composite VDF-TeFE/PVP scaffolds.

Starting with the FTIR spectrum of pure PVP, the absorption band is located around 1650 см$^{-1}$ can be ascribed to the stretching vibration of the C=O in the pyrrolidone group. The bands at 1421 cm^{-1} and 1372 cm^{-1} correspond to the CH deformation modes from the CH_2 group [23]. The peaks 1287 cm^{-1} are related to C–N bending vibration from the pyrrolidone structure. Small absorption band at about 1495 cm^{-1} refers to the characteristic vibration of C=N (pyridine ring) [24].

In the spectrum of a scaffold made of VDF-TeFE copolymer, two intense absorption bands are observed in the region of 1165 cm^{-1} and 1188 cm^{-1}, which are a superposition of twisting and stretching vibrations in the CH_2 and CF_2 groups, respectively. Intense absorption band in the 1398 cm^{-1} region corresponds to a superposition of wagging and antisymmetric stretching vibrations in the CH_2 and C-C groups. The band in the 884 cm^{-1} region is a superposition of antisymmetric stretching and rocking vibrations in the CF_2 group and rocking vibrations in the CH_2 group. An insignificant band in the region of 840 cm^{-1} is a superposition of symmetric stretching vibrations in the CF_2 and C-C groups [25,26].

The presence of intense bands in the region of 840, 884, and 1398 cm^{-1} corresponding to the trans-conformations with a slight band in the region of 925 cm^{-1} gauche-conformation indicates that macromolecules of the VDF-TeFE copolymer in the formed membranes have predominantly

Preprints (www.preprints.org) | NOT PEER-REVIEWED | Posted: 5 November 2020 doi:10.20944/preprints202011.0218.v1

a planar zigzag conformation with a strong dipole moment directed perpendicular to the axis of the polymer chain [27].

With an increase of the PVP content in the membranes and increase in the intensity of the bands in the range of 1650 cm^{-1}, 1495 cm^{-1}, 1421 cm^{-1}, 1372 cm^{-1} and 1287 cm^{-1} corresponding to PVP is observed. Whereas, the intensity of the bands in the range of 1165 cm^{-1}, 1188 cm^{-1}, 1398 cm^{-1}, 884 cm^{-1} and 840 cm^{-1} corresponding to the VDF-TeFE copolymer decreases. An increase in the PVP content in the formed membranes retains the conformation of a planar zigzag in the macromolecules of the VDF-TeFE copolymer, as evidenced by the presence of bands in the region of 840, 884, and 1398 cm^{-1} as well as the absence of shifts of these bands, regardless of the PVP content in the formed membranes. Whilst, in composite membranes, a shift of the band from the region of 1650 cm^{-1} (C = O in the pyrrolidone group) to the region of 1662 cm^{-1} is observed. Such shift may indicate dipole-dipole interactions between PVP and VDF-TeFE [28].

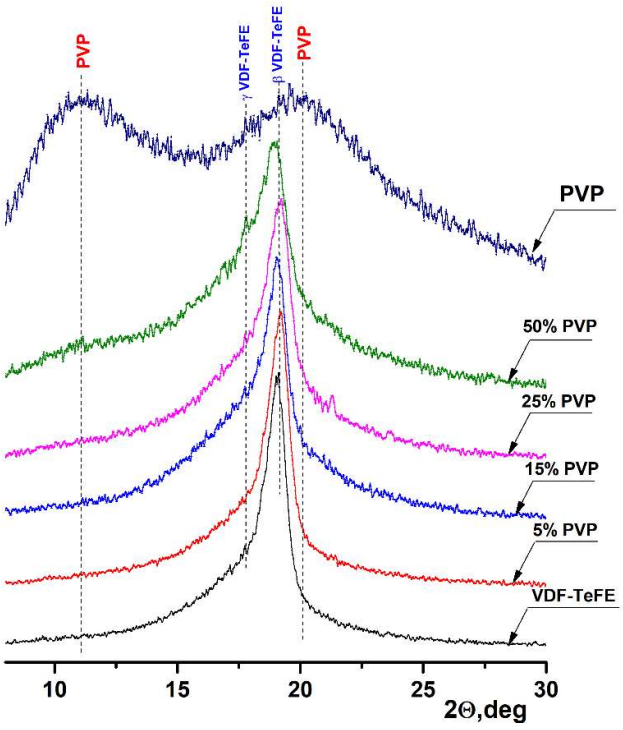

Figure 3. XRD pattern of the investigated samples.

The XRD patterns of the formed membranes are shown in Figure 3. The XRD pattern of pure PVP in the region of 10.9° and 21.5° shows two wide characteristic halo peaks, corresponding to the amorphous PVP [29]. An intensive peak at 19.2° on the XRD pattern of membranes formed from VDF-TeFE copolymer corresponds to the most electrically active ferroelectric β -phase of the VDF-TeFE copolymer formed by macromolecules in TTT conformation [30]. At the same time, a halo associated with the formation of an electrically active γ phase formed by macromolecules in the TTT conformation could be observed at 17.8°. The formation of electrically active crystalline phases is associated with high intensity of the electric field between the injector and the collector, high tensile forces from the electric field in process of the membranes formation [31] and the alignment effect of TeFE segments on the PVDF macromolecule [32]. With an increase of the PVP content, the half-width of the β-phase peak increases from 0.889° for pure VDF-TeFE membranes to 1.738° for VDF-TeFE membranes containing 50% PVP. The intensity of the halo reflection at 17.8° also increases, indicating difficulties of the electrically active β-phase crystallization process in VDF-

Preprints (www.preprints.org) | NOT PEER-REVIEWED | Posted: 5 November 2020 doi:10.20944/preprints202011.0218.v1

TeFE copolymer. It can be attributed to the penetration of PVP molecules into the VDF-TeFE structure and the formation of significant transition layers formed as a result of tensile forces from the electric field.

Images of cells on the surface of the cell culture plastic and VDF-TeFE membranes with different PVP content are shown in Figure 4.

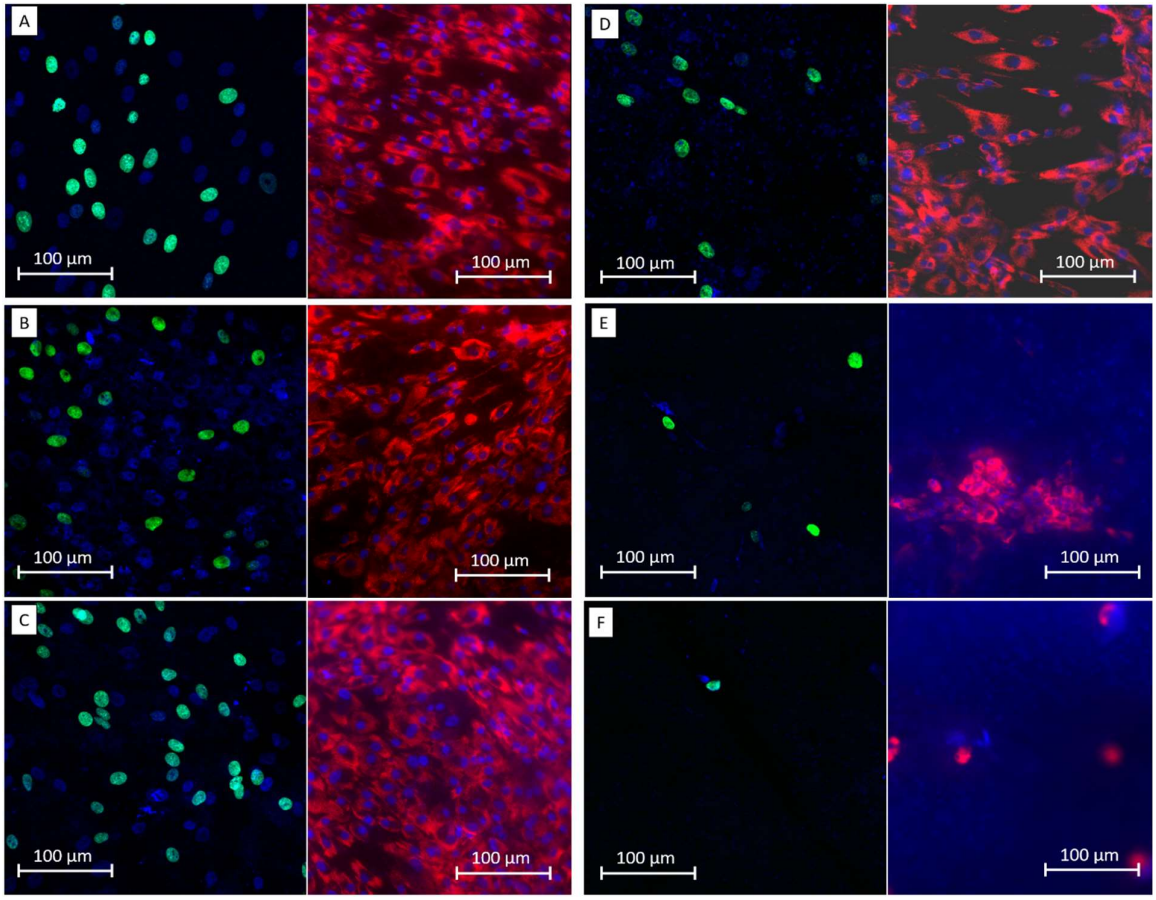

Figure 4. Images of cells on the surface of a-cell culture plastic, VDF-TeFE membranes with different PVP content: b -0%, c-5%, d-15%, e-25% f-50%.

The number of fibroblasts adhered to the surface of the cell culture plastic compared to the surface of the formed membranes was higher for all the studied groups (Table 3). The highest number of cells adhered onto scaffold surface was observed for VDF-TeFE membranes with a PVP content of 0 and 5 wt%. These samples were characterized by high viability and proliferation of adhered cells. Despite a significant decrease in the number of adherent cells for membranes with PVP content of 15 wt%, the viability and proliferation of fibroblasts on the did not significantly differ from the corresponding values for scaffold with lover PVP content. PVP content of 25 wt% or more led to a dramatic decrease of the viability and proliferation of fibroblasts on the surface of the membranes (Table 3).

Preprints (www.preprints.org) | NOT PEER-REVIEWED | Posted: 5 November 2020 doi:10.20944/preprints202011.0218.v1

Table 3. Cell citotoxity, adhesion and proliferation.

	Number of fibroblasts [pcs/mm^2]	Viability, %	Proliferation, %
	Me(Q1;Q3)		
Cell culture plastic	181 (145;207)	98 (95;99)	39 (23;49)
PVP,%			
0	146 (92; 190)*	97 (95;99)	19 (14;31)*,
5	141 (73; 177)*	96 (94;98)	22 (15;31)*
15	72 (49; 92)*,**	96 (94;99)	21 (6;41)*
25	5.5 (3.0;10.0) *,**	73 (63;81) *,**	11 (3;46) *,**
50	8.0 (5.5;13.0) *,**	68 (58;81) *,**	0 (0;8) *,**

*p < 0.05 compared to cell culture plastic.

**p < 0.05 compared to VDF-TeFE membranes with PVP content 0%.

The decrease in adhesion, viability and proliferation of fibroblasts with an increase in PVP content may be due to the following reasons. PVP is a water-soluble, hydrophilic polymer. Thus, PVP can diffuse into the culture medium [33]. The amount of PVP released into the culture medium over a certain period of time is determined by the content of PVP in the sample. It is known that PVP is protonated in aqueous solutions and can form complexes with anions, including various biologically active molecules [34]. Thus, an increase of PVP content may lead to an increase in the content of complexes with biologically active anions in the culture medium, changing its chemical composition and reducing the availability of anions for cells. On the other hand, diffused PVP in the culture medium can lead to its accumulation in cells causing “lysosomal storage disease” which inhibits the processes of vital activity of cells causing their death [35]. The third possible reason for a decrease in cell viability on the surface of membranes with a high content of PVP is the process of its leaching from the fibers leading to membrane deformation (supplementary file) preventing cell attachment to the scaffold surface [33]. And finally, the fourth reason could be the formation of toxic complexes between PVP and DMF during the spinning solution preparation, followed by its migration into the culture medium, which is indirectly evidenced by an increase in the concentration of DMF in the formed membranes with an increase in the concentration of PVP (Table 2).

It was shown that VDF-TeFE membranes containing 15 wt% PVP have optimal morphology, chemical, crystal structure, and are sufficiently capable of maintaining the necessary conditions for adhesion and proliferation of fibroblasts on their surface, which makes it possible

Preprints (www.preprints.org) | NOT PEER-REVIEWED | Posted: 5 November 2020 doi:10.20944/preprints202011.0218.v1

to use this type of membranes for pilot studies to explore the possibility of their use to restore the skin in the case of contaminated full-thickness wounds.

The contaminated full-thickness wound, wound treated with gauze dressing soaked in chlorhexidine solution, and wound treated with VDF-TeFE membrane containing 15 wt% PVP after 7 days are shown in Figure 5.

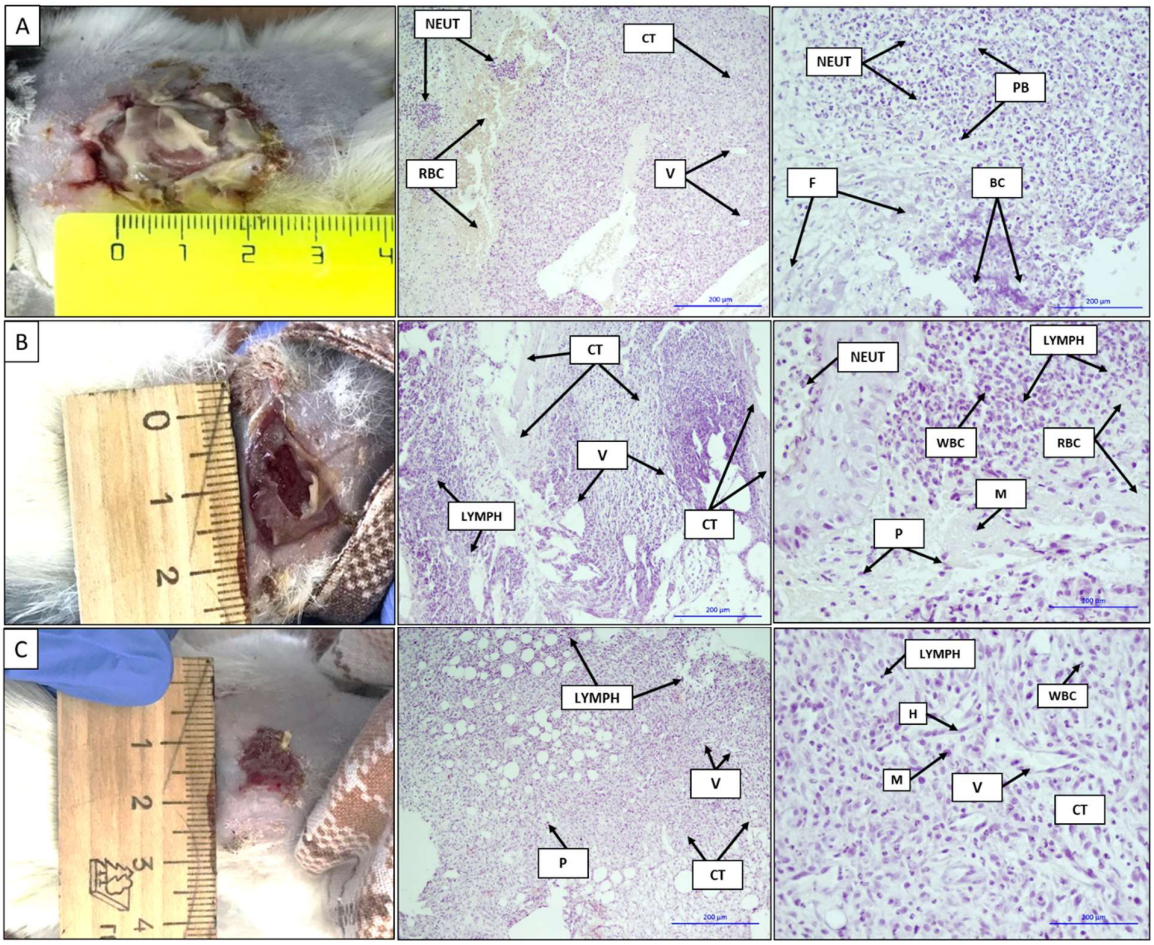

Figure 5. Images and histological sections of a - contaminated full-thickness wound, b - wound treated gauze dressing soaked in chlorhexidine solution and c - wound treated with VDF-TeFE membrane containing 15 wt% PVP on 7th day. V - vessels, H - histiocytes, NEUT - neutrophils, WBC - leukocytes, RBC - erythrocytes, CT - connective tissue, LYMPH - lymphocytes, M - macrophages, P - plasma cells, F - fibrin, Purulent bodies (PB) - purulent bodies, Bacterial colonies (BC) - colonies of bacteria. The bars corresponds to 200 μm.

The formed contaminated wound is a focus of acute purulent-necrotic inflammation, as evidenced by the gray-green color accompanied by characteristic unpleasant odor on the surface of the wound. The shape of the wound is circular with a diameter of ~ 2.5 cm (Figure 5a). Purulent inflammation with purulent bodies and large number of neutrophils hemorrhage foci were observed on histological sections. Basophilically stained structureless colonies of microorganisms

 doi:10.20944/preprints202011.0218.v1

are subtotally determined. Neutrophil infiltration into adipose tissue; erythrocytes, thin fibrin fibers, connective tissue with moderate lymphoid infiltration with the presence of leukocytes and neoangiogenesis; vasculitis and erythrocytes in the vascular lumen are observed (Fig. 5a).

The wound size treated with gauze bandage soaked in chlorhexidine solution decreased to 1.5 cm on the 7th day of the experiment. The bottom of the wound was covered with an abundant layer of fibrin, easily separated from the wound upon contact. An active formation of granulation tissue was observed under the fibrin layer (Figure 5B). On histological sections, mature and immature connective tissue with pronounced lymphoid infiltration and presence of vascular fissures is observed. On the periphery of the histological section an inflammation in the adipose tissue, represented by a large number of neutrophils with masses and filaments of fibrin, as well as bacterial colonies is observed. There is a pronounced neutrophilic infiltration with the presence of lymphoid cells and macrophages. On the left side of the image, a layer of stratified squamous epithelium with edema and the presence of neutrophils on its surface can be seen (Figure 5B).

In case of VDF-TeFE membrane containing 15% PVP wound treatment, the diameter of the wound decreased up to ~ 1 cm on the 7th day of the experiment. A slight granulation tissue appeared on the surface of the wound. An active epithelialization and tissue granulation were observed on the periphery of the wound. Histological sections are represented by fibrous-adipose tissue, pronounced neoangiogenesis and moderate lymphoid infiltration. Among the cellular infiltrate, single plasmocytes are determined. In the fibrous tissue, a heterogeneous cellular infiltrate is clearly defined, represented mainly by lymphohistiocytes and to a lesser extent by plasma cells, macrophages and neutrophils. Fibrous-adipose tissue with moderate lymphoid infiltration with the presence of plasma cells and single neutrophils; presence of vessels with an endothelial lining is observed (Figure 5C).

VDF-TeFE membrane containing 15% PVP shows better effect on skin healing in the case of contaminated full-thickness wound compared to standard gauze dressings impregnated with chlorhexidine. It might be due to following reasons. First, membranes made by electrospinning have interconnected porosity formed by micron-sized fibers resulting in significant free surface [36] and the ability of PVP to bind toxins and water [34]. These properties of the obtained membranes make it possible to absorb a significant amount of exudate released by pathogenic microflora, as well as maintain the required moisture level on the wound surface. The absorbed exudate saturated with pathogens is removed along with the membrane, thus reducing the concentration of pathogens with each subsequent dressing. In addition, PVP released from fibers into the exudate can accumulate in pathogenic cells causing “lysosomal storage disease” provoking their death [37]. Thus, the presence of PVP in fibers is a factor that reduces the concentration of pathogens in the regeneration zone.

Second, it is known that PVDF-based piezoelectric polymer membranes are capable of negatively affecting the *Staphylococcus* culture when under dynamic load the membrane even in the absence of antibacterial agents [38]. Since in membranes containing 15 wt% of PVP, the predominant conformation of VDF-TeFE macromolecules is the electrically active *trans* conformation (Figure 2) and crystallites with characteristic ferroelectric properties predominate in the crystal structure (Figure 3), it can be assumed that decrease in the concentration of pathogens in the wound and improved tissue regeneration is due to the piezoelectric properties of the formed membranes.

Third, it is known that under the influence of external mechanical stimuli piezoelectric membranes can enhance migration, adhesion, and cytokine secretion in NIH3T3 fibroblasts in vitro [39]. The capacity of piezoelectric membranes to generate electrical impulses in response to the mechanical action of the tissue surrounding the implant allows to promote the wound healing regardless of the implantation zone [40].

Thus, the piezoelectric properties of the formed membranes make it possible to enhance the processes of tissue regeneration.

4. Conclusion

Composite VDF-TeFE/PVP membranes with different PVP content have been successfully fabricated by electrospinning. It has been shown that regardless of the PVP concentration membranes are formed by randomly intertwining fibers providing interconnected porosity. An increase in the PVP content in spinning solutions leads to a decrease in the fiber diameter due to lower conductivity and dynamic viscosity of the solutions. Higher PVP concentration also results in an increase in the content of oxygen (O) and nitrogen (N) in the formed membranes while hindering crystallization process of the VDF-TeFE copolymer in the ferroelectric β-phase.

Cytotoxicity and proliferative activity of human fibroblasts cultured on the membranes surface decrease with an increase in PVP amount. It has been shown that the optimum PVP content in the spinning solution is 15 wt%. Studies of the healing process of contaminated full-thickness wounds show that compared to standard gauze dressings soaked in an aqueous solution of chlorhexidine composite VDF-TeFE/PVP membranes demonstrate a better healing effect.

Acknowledgments

Membranes fabrication, physicochemical properties and *in vivo* studies were funded by RFBR, project number # 20-03-00171.

In vitro studies of scaffolds was supported by the Complex Program of Basic Research under the Siberian Branch of the Russian Academy of Sciences within the Basic Research Topic of Research Institute for Complex Issues of Cardiovascular Diseases № 0546-2019-0002 "Pathogenetic basis for the development of cardiovascular implants from biocompatible materials using patient-oriented approach, mathematical modeling, tissue engineering, and genomic predictors".

References

[1] D. Chouhan, B.B. Mandal, Silk biomaterials in wound healing and skin regeneration therapeutics: From bench to bedside, Acta Biomater. 103 (2020) 24–51. https://doi.org/10.1016/j.actbio.2019.11.050.

[2] N. Mayet, Y.E. Choonara, P. Kumar, L.K. Tomar, C. Tyagi, L.C. Du Toit, V. Pillay, A Comprehensive Review of Advanced Biopolymeric Wound Healing Systems, J. Pharm. Sci. 103 (2014) 2211–2230. https://doi.org/10.1002/jps.24068.

[3] G.T. Lionelli, W.T. Lawrence, Wound dressings, Surg. Clin. North Am. 83 (2003) 617–638. https://doi.org/10.1016/S0039-6109(02)00192-5.

[4] D. Chouhan, N. Dey, N. Bhardwaj, B.B. Mandal, Emerging and innovative approaches for wound healing and skin regeneration: Current status and advances, Biomaterials. 216 (2019) 119267. https://doi.org/10.1016/j.biomaterials.2019.119267.

[5] S.P. Miguel, D.R. Figueira, D. Simões, M.P. Ribeiro, P. Coutinho, P. Ferreira, I.J. Correia, Electrospun polymeric nanofibres as wound dressings: A review, Colloids Surfaces B Biointerfaces. 169 (2018) 60–71. https://doi.org/10.1016/j.colsurfb.2018.05.011.

[6] A.D. Juncos Bombin, N.J. Dunne, H.O. McCarthy, Electrospinning of natural polymers for the production of nanofibres for wound healing applications, Mater. Sci. Eng. C. 114 (2020) 110994. https://doi.org/10.1016/j.msec.2020.110994.

[7] R.S. Ambekar, B. Kandasubramanian, Advancements in nanofibers for wound dressing: A review, Eur. Polym. J. 117 (2019) 304–336. https://doi.org/10.1016/j.eurpolymj.2019.05.020.

[8] M. Minary-Jolandan, M.-F. Yu, Nanoscale characterization of isolated individual type I collagen fibrils: polarization and piezoelectricity, Nanotechnology. 20 (2009) 085706. https://doi.org/10.1088/0957-4484/20/8/085706.

[9] C. Ning, Z. Zhou, G. Tan, Y. Zhu, C. Mao, Electroactive polymers for tissue regeneration: Developments and perspectives, Prog. Polym. Sci. 81 (2018) 144–162. https://doi.org/10.1016/j.progpolymsci.2018.01.001.

[10] A. Marino, G.G. Genchi, E. Sinibaldi, G. Ciofani, Piezoelectric Effects of Materials on Bio-Interfaces, ACS Appl. Mater. Interfaces. 9 (2017) 17663–17680. https://doi.org/10.1021/acsami.7b04323.

[11] M. Han, H. Wang, Y. Yang, C. Liang, W. Bai, Z. Yan, H. Li, Y. Xue, X. Wang, B. Akar, H. Zhao, H. Luan, J. Lim, I. Kandela, G.A. Ameer, Y. Zhang, Y. Huang, J.A. Rogers, Three-dimensional piezoelectric polymer microsystems for vibrational energy harvesting, robotic interfaces and biomedical implants, Nat. Electron. 2 (2019) 26–35. https://doi.org/10.1038/s41928-018-0189-7.

[12] C. Ribeiro, V. Sencadas, D.M. Correia, S. Lanceros-Méndez, Piezoelectric polymers as biomaterials for tissue engineering applications, Colloids Surfaces B Biointerfaces. 136 (2015) 46–55. https://doi.org/10.1016/j.colsurfb.2015.08.043.

[13] K.S. Ramadan, D. Sameoto, S. Evoy, A review of piezoelectric polymers as functional materials for electromechanical transducers, Smart Mater. Struct. 23 (2014) 033001. https://doi.org/10.1088/0964-1726/23/3/033001.

[14] A. Venault, K.-H. Lin, S.-H. Tang, G.V. Dizon, C.-H. Hsu, I.V.B. Maggay, Y. Chang, Zwitterionic electrospun PVDF fibrous membranes with a well-controlled hydration for diabetic wound recovery, J. Memb. Sci. 598 (2020) 117648. https://doi.org/10.1016/j.memsci.2019.117648.

[15] S. Du, N. Zhou, Y. Gao, G. Xie, H. Du, H. Jiang, L. Zhang, J. Tao, J. Zhu, Bioinspired hybrid patches with self-adhesive hydrogel and piezoelectric nanogenerator for promoting skin wound healing, Nano Res. (2020). https://doi.org/10.1007/s12274-020-2891-9.

[16] T. He, J. Wang, P. Huang, B. Zeng, H. Li, Q. Cao, S. Zhang, Z. Luo, D.Y.B. Deng, H. Zhang, W. Zhou, Electrospinning polyvinylidene fluoride fibrous membranes containing anti-bacterial drugs used as wound dressing, Colloids Surfaces B Biointerfaces. 130 (2015) 278–286. https://doi.org/10.1016/j.colsurfb.2015.04.026.

[17] A.D. Badaraev, A. Koniaeva, S.A. Krikova, E.V. Shesterikov, E.N. Bolbasov, A.L. Nemoykina, V.M. Bouznik, K.S. Stankevich, Y.M. Zhukov, I.P. Mishin, E.Y. Varakuta, S.I. Tverdokhlebov, Piezoelectric polymer membranes with thin antibacterial coating for the regeneration of oral mucosa, Appl. Surf. Sci. 504 (2020) 144068. https://doi.org/10.1016/j.apsusc.2019.144068.

[18] Z. Cui, E. Drioli, Y.M. Lee, Recent progress in fluoropolymers for membranes, Prog. Polym. Sci. 39 (2014) 164–198. https://doi.org/10.1016/j.progpolymsci.2013.07.008.

[19] Z. Cui, N.T. Hassankiadeh, Y. Zhuang, E. Drioli, Y.M. Lee, Crystalline polymorphism in poly(vinylidenefluoride) membranes, Prog. Polym. Sci. 51 (2015) 94–126. https://doi.org/10.1016/j.progpolymsci.2015.07.007.

[20] P. Martins, A.C. Lopes, S. Lanceros-Mendez, Electroactive phases of poly(vinylidene fluoride): Determination, processing and applications, Prog. Polym. Sci. 39 (2014) 683–706. https://doi.org/10.1016/j.progpolymsci.2013.07.006.

[21] H.W. C.G. Janet, R.W. Barbee, J.T. Bielitzki, L.A. Clayton, J.C. Donovan, C.F.M. Hendriksen, D.F. Kohn, N.S. Lipman, P.A. Locke, J. Melcher, F.W. Quimby, P.V. Turner, G.A. Wood, Guide for the care and use of laboratory animals, National Academies Press, Washington DC, 2011.

[22] R.J. Sengwa, S. Sankhla, Dielectric Dispersion Study of Poly(vinyl Pyrrolidone)–Polar Solvent Solutions in the Frequency Range 20 Hz–1 MHz, J. Macromol. Sci. Part B. 46 (2007) 717–747. https://doi.org/10.1080/00222340701388938.

[23] I.A. Safo, M. Werheid, C. Dosche, M. Oezaslan, The role of polyvinylpyrrolidone (PVP) as a capping and structure-directing agent in the formation of Pt nanocubes, Nanoscale Adv. 1 (2019) 3095–3106. https://doi.org/10.1039/C9NA00186G.

[24] A.M. Abdelghany, E.M. Abdelrazek, S.I. Badr, M.A. Morsi, Effect of gamma-irradiation on (PEO/PVP)/Au nanocomposite: Materials for electrochemical and optical applications, Mater. Des. 97 (2016) 532–543. https://doi.org/10.1016/j.matdes.2016.02.082.

[25] M. Kobayashi, K. Tashiro, H. Tadokoro, Molecular Vibrations of Three Crystal Forms of Poly(vinylidene fluoride), Macromolecules. 8 (1975) 158–171. https://doi.org/10.1021/ma60044a013.

[26] K. Tashiro, Y. Abe, M. Kobayashi, Computer simulation of structure and ferroelectric phase transition of vinylidene fluoride copolymers (1) vdf content dependence of the crystal structure, Ferroelectrics. 171 (1995) 281–297. https://doi.org/10.1080/00150199508018440.

[27] V. V Kochervinskii, The properties and applications of fluorine-containing polymer films with piezo- and pyro-activity, Russ. Chem. Rev. 63 (1994) 367–371.

https://doi.org/10.1070/RC1994v063n04ABEH000090.

[28] Prateek, R. Bhunia, A. Garg, R.K. Gupta, Poly(vinylpyrrolidone)/Poly(vinylidene fluoride) as Guest/Host Polymer Blends: Understanding the Role of Compositional Transformation on Nanoscale Dielectric Behavior through a Simple Solution–Process Route, ACS Appl. Energy Mater. 2 (2019) 6146–6152. https://doi.org/10.1021/acsaem.9b01092.

[29] W.H. Eisa, E. Al-Ashkar, S.M. El-Mossalamy, S.S.M. Ali, PVP induce self-seeding process for growth of Au@Ag core@shell nanocomposites, Chem. Phys. Lett. 651 (2016) 28–33. https://doi.org/10.1016/j.cplett.2016.03.009.

[30] A.J. Lovinger, D.D. Davis, R.E. Cais, J.M. Kometani, Compositional variation of the structure and solid-state transformations of vinylidene fluoride/tetrafluoroethylene copolymers, Macromolecules. 21 (1988) 78–83. https://doi.org/10.1021/ma00179a017.

[31] G. Kang, Y. Cao, Application and modification of poly(vinylidene fluoride) (PVDF) membranes – A review, J. Memb. Sci. 463 (2014) 145–165. https://doi.org/10.1016/j.memsci.2014.03.055.

[32] J.B. Lando, W.W. Doll, The polymorphism of poly(vinylidene fluoride). I. The effect of head-to-head structure, J. Macromol. Sci. Part B. 2 (1968) 205–218. https://doi.org/10.1080/00222346808212449.

[33] G.-M. Kim, K.H.T. Le, S.M. Giannitelli, Y.J. Lee, A. Rainer, M. Trombetta, Electrospinning of PCL/PVP blends for tissue engineering scaffolds, J. Mater. Sci. Mater. Med. 24 (2013) 1425–1442. https://doi.org/10.1007/s10856-013-4893-6.

[34] C.L. Burnett, PVP (Polyvinylpyrrolidone), Int. J. Toxicol. 36 (2017) 50S-51S. https://doi.org/10.1177/1091581817716649.

[35] R. Duncan, S.C.W. Richardson, Endocytosis and Intracellular Trafficking as Gateways for Nanomedicine Delivery: Opportunities and Challenges, Mol. Pharm. 9 (2012) 2380–2402. https://doi.org/10.1021/mp300293n.

[36] J. Ding, J. Zhang, J. Li, D. Li, C. Xiao, H. Xiao, H. Yang, X. Zhuang, X. Chen, Electrospun polymer biomaterials, Prog. Polym. Sci. 90 (2019) 1–34. https://doi.org/10.1016/j.progpolymsci.2019.01.002.

[37] V. Milosavljevic, P. Jelinkova, A.M. Jimenez Jimenez, A. Moulick, Y. Haddad, H. Buchtelova, S. Krizkova, Z. Heger, L. Kalina, L. Richtera, P. Kopel, V. Adam, Alternative Synthesis Route of Biocompatible Polyvinylpyrrolidone Nanoparticles and Their Effect on Pathogenic Microorganisms, Mol. Pharm. 14 (2017) 221–233. https://doi.org/10.1021/acs.molpharmaceut.6b00807.

[38] E.O. Carvalho, M.M. Fernandes, J. Padrao, A. Nicolau, J. Marqués-Marchán, A. Asenjo, F.M. Gama, C. Ribeiro, S. Lanceros-Mendez, Tailoring Bacteria Response by Piezoelectric Stimulation, ACS Appl. Mater. Interfaces. 11 (2019) 27297–27305. https://doi.org/10.1021/acsami.9b05013.

[39] H.-F. Guo, Z.-S. Li, S.-W. Dong, W.-J. Chen, L. Deng, Y.-F. Wang, D.-J. Ying, Piezoelectric PU/PVDF electrospun scaffolds for wound healing applications, Colloids Surfaces B Biointerfaces. 96 (2012) 29–36. https://doi.org/10.1016/j.colsurfb.2012.03.014.

[40] A. Wang, Z. Liu, M. Hu, C. Wang, X. Zhang, B. Shi, Y. Fan, Y. Cui, Z. Li, K. Ren, Piezoelectric nanofibrous scaffolds as in vivo energy harvesters for modifying fibroblast alignment and proliferation in wound healing, Nano Energy. 43 (2018) 63–71. https://doi.org/10.1016/j.nanoen.2017.11.023.